E-Plane Steps in Rectangular Waveguide

Tullio Rozzi, *Fellow*, *IEEE*, and Mauro Mongiardo

Abstract—**In this paper, the classical problem of interacting *E*-plane step discontinuities is reconsidered. New, frequency-independent equivalent circuits are derived by explicitly considering the edge condition in the rigorous Ritz–Galerkin variational approach. A dramatic reduction of the numerical effort has also been achieved; in fact, in no case were more than two basis functions needed. The theoretical results have been compared with those reported in [1] as well as with experimental tests, always with excellent agreement. The very high accuracy, the reduced numerical effort, and the absence of relative convergence phenomena make this method ideally suited for the full-wave analysis of interacting discontinuities in efficient CAD routines for small desk-top computers.**

I. Introduction

WAVEGUIDE *E*-plane step discontinuities still find many applications in millimetric and in microwave practice as building blocks for filters, matching networks, branch line couplers, phase shifters, etc. Although this subject is often considered a "mature" one, a look at the technical literature reveals continuing interest. In fact, the synthesis of the aforementioned components is often based on computer optimization routines which require repeated wide-band analysis of cascaded interacting step discontinuities. In addition, the widespread availability of desktop computer facilities promotes very efficient codes capable of performing the synthesis process on such machines.

In the present paper the *E*-plane step discontinuity problem has been reconsidered using the viewpoint of the wide-band equivalent networks with frequency-independent elements given in [2]. The present formulation, however, is easier to derive while allowing accommodation for the correct edge singularity of the field.

Some overall remarks on the most widely used techniques are possible when one considers that many analytical methods used to solve waveguide discontinuity problems start from the same integral equation [3]. The latter is obtained by imposing the boundary conditions on the transverse components of the electromagnetic fields at the two sides of the discontinuity. To solve the resulting integral equation, several different possibilities are at hand. In [1] and [4] it was solved with the application of the equivalent static method, which consists in obtaining an analogous integral equation for the static case. By resorting to conformal mapping, static solutions are then available, and by again using the analogy, the solution to the original problem can be found. It should be remarked that solutions obtained with this method are often fairly accurate, and an example of this will be given in Table II. Unfortunately, the following drawbacks are also present:

- the results are valid only on a limited range of frequencies;
- the equivalent circuit elements are frequency-dependent;
- interacting discontinuities are not considered;
- since the method is based on conformal mapping, it can be applied only to two-dimensional discontinuity problems not involving dielectrics.

It should be kept in mind that this ingenious, but analitically cumbersome, method to solve the integral equation was followed by Schwinger in order to overcome the lack of computing facilities at the time. Nowadays, with the wide diffusion of such resources, techniques based on the moment method have became increasingly popular. In particular, if we expand the unknown in terms of normal modes and use the Galerkin method, the mode-matching formulation is recovered [3]. However, the apparent simplicity of this method conceals certain difficulties. In fact, in order to obtain accurate solutions, the number of terms used to express the unknown must be quite high. Moreover this number should be related to the number of terms retained when truncating the Green's function, the relationship being given by the geometrical ratio of the discontinuity [5]. In conclusion the main disadvantages of using mode-matching techniques are:

- the impossibility of deriving an equivalent circuit;
- the inversion of a matrix of relatively large dimension;
- the relative convergence phenomenon.

The method presented here combines the simplicity of the mode-matching formulation with the accuracy of the equivalent static method, making use of the framework of the variational approach. The expanding functions, however, are selected so as to satisfy the static edge conditions and no phenomenon of relative convergence exists; neither is any restriction arising from the geometrical parameters of the structure present.

Taking advantage of previous works [2], it is possible to draw simple and accurate wide-band network models not

Manuscript received September 17, 1990; revised March 26, 1991.

T. Rozzi is with the Dipartimento di Elettronica ed Automatica, Università di Ancona, Via Brecce Bianche, 60100 Ancona, Italy.

M. Mongiardo is with the Dipartimento di Ingegneria Elettronica, Università "Tor Vergata," Via O. Raimondo, 00173 Roma, Italy.

IEEE Log Number 9101022.

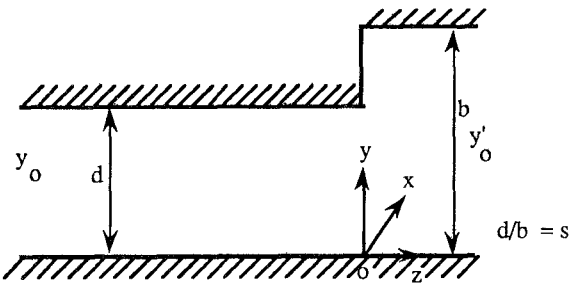

Fig. 1. Geometry of the E-plane step.

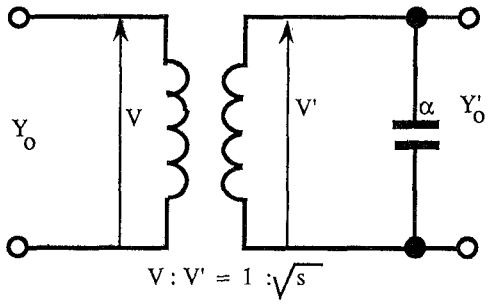

Fig. 2. Equivalent circuit of the step.

only for the single discontinuity, but also for cascaded strongly interacting discontinuities. Since even in interacting discontinuities only the modes above cutoff or just below cutoff, but still "tunneling" to the next discontinuity, i.e., the "accessible" modes, produce the interaction, it seems natural to use a scattering matrix description of just the accessible modes. A variational expression for the scattering matrix has therefore been derived.

II. Approximate Theory for the Isolated Step Discontinuity in Monomode Waveguide

The geometry of the step is shown in Fig. 1 in longitudinal section. The fundamental TE_{10} mode only is propagating in both waveguides with the same propagation constant β. The admittance of the fundamental TE mode,

$$Y_0 = \frac{\omega \epsilon_0}{\beta} \tag{1}$$

is the same in both waveguides. However, in order to ensure continuity of the dc voltage at the step, the characteristic admittance of the transmission line representing the larger guide is effectively set equal to

$$Y_0' = sY_0$$

where $s = d/b < 1$ is the step ratio. This change of admittance level can be modeled by means of an ideal transformer of ratio $1:\sqrt{s}$, while retaining unit admittance at both ports. It is, moreover, convenient to normalize Y_0 to unity and to introduce an "effective" frequency variable for the problem, defined as

$$u = \frac{\beta b}{\pi} = \frac{2b}{\lambda_g}$$

such that $u = 0$ at cutoff of the fundamental mode in the larger guide and $u = 1$ at that of the first higher order mode (LSE_{11}). It is physically obvious that the energy storage from higher order modes which takes place mainly in the larger waveguide is mainly capacitive and that in view of the transverse nature of the discontinuity, it can be represented by a shunt element.

Consequently, the equivalent circuit of Fig. 2 is in principle an accurate description of the discontinuity. Clearly, the capacitance α is still a function of the frequency u, as well as of the step ratio.

From [1] we derive the following approximations for α:

$$\alpha = 2 \ln \frac{e}{4s}, \qquad s \ll 1: \text{large step} \tag{2a}$$

$$= \frac{(1-s)^2}{2s} \ln \frac{2}{1-s}, \qquad s \approx 1: \text{small step.} \tag{2b}$$

More accurate expressions for α require a rigorous field solution, such as will be provided in the following. From the equivalent circuit of Fig. 2, elementary network analysis yields the two-port scattering matrix of the step with elements

$$S_{11} = \frac{1 - s - j\alpha us}{1 + s + j\alpha us} \tag{3a}$$

$$S_{22} = -\frac{1 - s + j\alpha us}{1 + s + j\alpha us} \tag{3b}$$

$$S_{12} = \frac{2\sqrt{s}}{1 + s + j\alpha us}. \tag{3c}$$

It is apparent from (3a)–(3c) that $(|S_{11}|) = (|S_{22}|)$. Moreover, when the effect of higher order modes is neglected ($\alpha = 0$), the well-known approximation for a small step is recovered, namely

$$S_{11} = \frac{1-s}{1+s} = -S_{22}. \tag{4}$$

III. Rigorous Theory of the Asymmetric E-Plane Step

With reference to Fig. 1, a TE_{10} mode incident on the discontinuity excites higher order LSE_{1n}^x modes, which can be derived in each region from an x-directed magnetic vector potential of the type

$$\Pi_h = \sin \frac{\pi x}{a} \sum_{n=0,1,} \alpha_n \varphi_n(y) e^{-\gamma_n z}.$$

The uniform x dependence does not enter the problem and can be factored out. E_y and H_x provide a pair of fields transverse to the discontinuity that can be derived from the above potential [6].

Within an arbitrary constant, the y dependence of the fields is as follows:

$$\varphi_n(y) = \sqrt{\frac{\epsilon_n}{d}} \cos \frac{n\pi y}{d} \tag{5a}$$

$$\psi_n(y) = \sqrt{\frac{\epsilon_n}{b}} \cos \frac{n\pi y}{b} \tag{5b}$$

where

$$\epsilon_n = 2, \qquad n > 0$$
$$\epsilon_n = 1, \qquad n = 0$$

corresponding to the propagation constants

$$\gamma_n = \left[\left[\frac{n\pi}{d}\right]^2 + \left[\frac{\pi}{a}\right]^2 - \left[\frac{2\pi}{\lambda}\right]^2\right]^{1/2} \tag{6a}$$

$$\gamma'_n = \left[\left[\frac{n\pi}{b}\right]^2 + \left[\frac{\pi}{a}\right]^2 - \left[\frac{2\pi}{\lambda}\right]^2\right]^{1/2}. \tag{6b}$$

Normalizing all modal admittances to that of the fundamental mode, we have

$$sY_0 = Y'_0 = 1$$

in both guides and, for $n > 0$,

$$Y_n = \frac{j\beta}{\gamma_n} \qquad \text{in guide } d$$

$$Y'_n = \frac{j\beta}{\gamma'_n} \qquad \text{in guide } b.$$

The continuity of the transverse field E_y, H_x at $z = 0$ is expressed as

$$E_y = \sum_{n=0}^{p-1} A_n\varphi_n + \sum_{n=0}^{\infty} B_n\varphi_n \tag{7a}$$

$$= \sum_{n=0}^{q-1} A'_n\psi_n + \sum_{n=0}^{\infty} B'_n\psi_n \tag{7b}$$

$$-H_x = \sum_{n=0}^{p-1} Y_nA_n\varphi_n - \sum_{n=0}^{\infty} Y_nB_n\varphi_n \tag{8a}$$

$$= -\sum_{n=0}^{q-1} Y'_nA'_n\psi_n + \sum_{n=0}^{\infty} Y'_nB'_n\psi_n. \tag{8b}$$

It is noted that p $(n = 0, \cdots, p-1)$ modes are considered as possibly incident and "accessible" in guide d, and q in guide b. The remaining modes are only present as reflected waves. Hence, by orthogonality, we have from (7)

$$\begin{aligned} B_n &= \langle E_y, \varphi_n\rangle - A_n \\ A_n &= 0, \qquad n \geqslant p \\ B'_n &= \langle E_y, \psi_n\rangle - A'_n \\ A'_n &= 0, \qquad n \geqslant q. \end{aligned} \tag{9}$$

Hence, by inserting (9) into (8), we obtain the integral equation for the electric field $E = E_y$ of the discontinuity:

$$\sum_{n=0}^{p-1} Y_nA_n\varphi_n + \sum_{n=0}^{q-1} Y'_nA'_n\psi_n = \hat{Y}E = \int_0^d Y(y, y')E(y')\,dy' \tag{10}$$

where $\hat{Y}$ is the integral operator whose kernel is the Green's admittance function in the scattering representation, i.e.,

$$Y(y, y') = \frac{1}{2}\sum_{n=0}^{\infty} Y_n\varphi_n(y)\varphi_n(y') + \frac{1}{2}\sum_{n=0}^{\infty} Y'_n\psi_n(y)\psi_n(y'). \tag{11}$$

In order to derive the $(p+q)\times(p+q)$ scattering matrix S for the junction, let us furthermore scale and relabel the incident and reflected voltage waves in the usual manner, i.e., so that the ports are in sequential order and the characteristic admittance of each port is unity, as in Fig. 3, i.e.,

$$\begin{aligned} a_{n+1}(\text{or } b_{n+1}) &= Y_n^{1/2}A_n(\text{or } B_n), \quad 0 \leqslant n \leqslant p-1 \\ a_{n+1}(\text{or } b_{n+1}) &= Y'^{1/2}_{n-p+1}A'_{n-p+1}(\text{or } B'_n), \\ & \qquad p \leqslant n \leqslant p+q-1. \end{aligned} \tag{12}$$

It is noted that the above scaling of the admittance at the ports becomes complex for ports corresponding to an accessible mode below cutoff. This inconvenience may be avoided by using the original unscaled quantities and introducing unit termination only when computing real powers.

The scattering matrix S for the junction shown in Fig. 3 is defined by the linear relationship

$$\boldsymbol{b} = \boldsymbol{S}\boldsymbol{a}. \tag{13}$$

By linearity, the elements of the scattering matrix are

$$S_{ik} = b_i, \qquad a_k = 1; \quad a_{j\neq k} = 0.$$

Introducing the above excitations then in the form (12) for each port k $(1 \leqslant k \leqslant p+q)$ in the integral equation (10), one obtains $p+q$ integral equations for the unknown fields E_k set up at the discontinuity by these excitations:

$$\eta_k^{1/2}g_k = \hat{Y}E_k, \qquad 1 \leqslant k \leqslant p+q \tag{14}$$

where

$$\begin{aligned} g_k &= \varphi_{k-1}, \qquad 1 \leqslant k \leqslant p \\ g_k &= \psi_{k-p}, \qquad p+1 \leqslant k \leqslant p+q \end{aligned} \tag{15}$$

and η_k is the corresponding admittance. Hence, E_k can

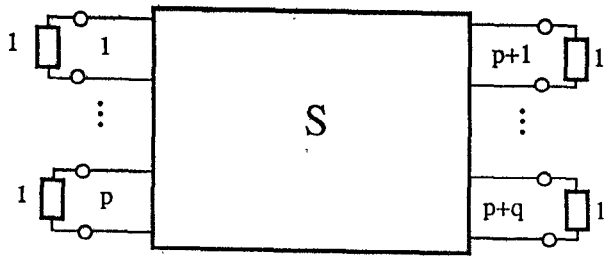

Fig. 3. Generalized scattering matrix.

be written formally by means of the inverse operator $\hat{Y}^{-1}$, or

$$E_k = \hat{Y}^{-1}\eta_k^{1/2} g_k. \tag{16}$$

By virtue of (9) and (12), however, we can now rewrite (14) as

$$\begin{aligned} S_{ik} = b_i &= \eta_i^{1/2}\langle g_i, E_k\rangle - \delta_{ik} \\ &= \eta_i^{1/2}\langle g_i, \hat{Y}^{-1} g_k\rangle \eta_k^{1/2} - \delta_{ik} \end{aligned} \tag{17}$$

which is the desired variational expression for the scattering matrix.

IV. Discretization of the Integral Equation

Application of the Galerkin method requires discretization of the integral equations (14) by means of an appropriate, preferably orthonormal, set of expanding functions. On account of the edge condition $r^{-1/3}$ on E_x at the 90° corner, we choose to employ for this purpose the Gegenbauer polynomials

$$C_m^{\upsilon}\left[\frac{y}{d}\right]$$

with υ such that the weighting function $w(y)$ appearing in the orthogonality integral [7] represents the above edge condition, namely

$$w(y) = \left[1 - \left[\frac{y}{d}\right]^2\right]^{\upsilon - 1/2} = \left[1 - \left[\frac{y}{d}\right]^2\right]^{-1/3}.$$

Hence $\upsilon = 1/6$ and, furthermore, as $dE/dy = 0$ at $y = 0$, we restrict the parity of the polynomials to be even. The resulting expansion functions, orthonormal in the interval $0 \leqslant y \leqslant d$ with respect to the weighting function w, are therefore

$$f_m(y) = \frac{1}{\sqrt{d}} \frac{1}{N_m} C_{2m}^{1/6}\left[\frac{y}{d}\right], \qquad m = 0, 1, \cdots, N-1 \tag{18}$$

the normalization factor N_m being given in Appendix I. We can now expand the unknown fields E_k as a finite series of the f_m, with unknown coefficients, of the form

$$E_k(y) = w(y) \sum_{m=0}^{N-1} \lambda_{mk} f_m(y). \tag{19}$$

The factor $w(y)$ takes care of the edge condition at $y = d$.

Let us correspondingly expand the known ϕ_n, ψ_n as a series of f_m, i.e.,

$$\varphi_n(y) = \sum_{m=0}^{N-1} P_{mn} f_m(y) \tag{20}$$

with

$$P_{mn} = \int_0^d f_m(y) w(y) \varphi_n(y)\, dy = \langle f_m, w\varphi_n\rangle \tag{21}$$

and

$$\psi_n(y) = \sum_{m=0}^{N-1} Q_{mn} f_m(y) \tag{22}$$

with

$$Q_{mn} = \langle f_m, w\psi_n\rangle. \tag{23}$$

The kernel $Y(y, y')$ of the integral equation can now be expressed as

$$Y(y, y') = \sum_{m,k=0}^{N-1} Y_{mk} f_m(y) f_k(y') \tag{24}$$

with

$$Y_{mk} = \frac{1}{2} \sum_{n=0}^{\infty} Y_n P_{mn} P_{kn} + \frac{1}{2} \sum_{n=0}^{\infty} Y_n' Q_{mn} Q_{kn}. \tag{25}$$

As a result of the expansions (19), (20), and (22), the unknown E_k corresponds to the N-dimensional column vector $\boldsymbol{\lambda}_k$; the known functions ψ_n, φ_n correspond to the vectors $\boldsymbol{P}_k, \boldsymbol{Q}_k$, respectively, whose elements are given by (21) and (23); G_k corresponds to g_k; and the integral operator $\hat{Y}$ corresponds to the matrix $\underline{Y}$ given elementwise by (25). The integral equations (14) are now discretized into the set of matrix equations

$$\eta_k^{1/2} \boldsymbol{G}_k = \underline{Y} \cdot \boldsymbol{\lambda}_k, \qquad 1 \leqslant k \leqslant p + q \tag{26}$$

which are numerically invertible and lead via (17) to the desired variational expression for the scattering matrix:

$$S_{ik} = \eta_i^{1/2} \boldsymbol{G}_i^T \cdot \boldsymbol{Y}^{-1} \cdot \boldsymbol{G}_k \eta_k^{1/2} - \delta_{ik} \qquad (1 \leqslant i, \quad k \leqslant p + q). \tag{27}$$

This expression needs recomputation at each spot frequency ω.

V. Frequency Dependence

It is stressed that vectors P and Q above are frequency-independent. They are functions only of the step ratio, $s = d/b$ $(0 < s < 1)$. Frequency enters (25) only through the modal characteristic admittances. In particular, for u large, the latter tend to their quasi-static limit. We have, then, in terms of u, for modes below cutoff,

$$Y_n' = \frac{1}{n} \frac{ju}{\sqrt{1 - \dfrac{u^2}{n^2}}} \approx \frac{ju}{n}, \qquad n \gg u \tag{28}$$

$$Y_n = \frac{1}{n} \frac{jsu}{\sqrt{1 - \left(\dfrac{su}{n}\right)^2}} \approx \frac{jsu}{n}, \qquad n \gg u. \tag{29}$$

In fact, a better approximation, one valid over the waveguide band, is obtained by continuous fraction expansion

$$Y_n = \frac{1}{n}\frac{ju}{\sqrt{1-\left(\frac{u}{n}\right)^2}} \Rightarrow \quad C_s = \frac{1}{3n} \quad L = \frac{9}{8n} \quad C = \frac{2}{3n}$$

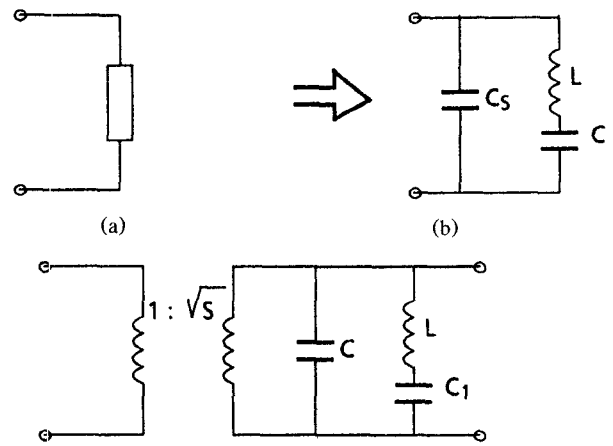

$$C = K\left[\frac{1}{3}\frac{J_{1/6}^2(\pi s)}{(\pi s)^{1/3}} + \sum_{n=2}^{\infty}\frac{1}{n^2}\frac{J_{1/6}^2(n\pi s)}{(\pi s)^{1/3}} + \sum_{n=1}^{\infty}\frac{1}{n^2}\frac{J_{1/6}^2(n\pi)}{(n\pi)^{1/3}}\right]$$

$$C_1 = \frac{2}{3}K\frac{J_{1/6}^2(\pi s)}{(\pi s)^{1/3}}$$

$$L\,C_1 = \frac{3}{4} \qquad K = \frac{2^{1/3}\,\Gamma^2\left(\frac{1}{6}\right)}{36} \approx 1.0849$$

(c)

Fig. 4. (a) Frequency-dependent capacitor; (b) lumped frequency-independent LC ring; (c) equivalent circuit of the step discontinuity.

of the square root up to second order, i.e.,

$$Y_n' \approx \frac{1}{3}\frac{ju}{n} + \frac{\frac{2}{3}\frac{ju}{n}}{1-\frac{3}{4}\frac{u^2}{n^2}} \tag{30a}$$

$$Y_n \approx \frac{1}{3}\frac{jsu}{n} + \frac{\frac{2}{3}\frac{jsu}{n}}{1-\frac{3}{4}\left[\frac{us}{n}\right]^2} = \frac{1}{3}\frac{jsu}{n}\left[1+\frac{2}{1-\frac{3}{4}\left(\frac{us}{n}\right)^2}\right]. \tag{30b}$$

Consequently, $Y_n'(u)$ is representable exactly as the frequency-dependent capacitor of Fig. 4(a) or, to a high degree approximation, by the lumped frequency-independent LC ring of Fig. 4(b). Depending on p, q and the ratio s, it may be quite sufficient to replace all admittances by their quasi-static limit.

If only the fundamental mode is propagating at either side of the step and the dynamic behavior of the first higher order mode of the large guide only is retained, we have then from (25), (29), and Appendix I the following Y matrix with explicit frequency and step-ratio dependence:

$$Y_{mk}(u,s) = \frac{1}{2}(1+s)P_{00}^2\delta_{m0}\delta_{k0} + \frac{ju}{2}\left[\left[\frac{1}{3}+\frac{\frac{2}{3}}{1-\frac{3}{4}u^2}\right]Q_{m1}(s)Q_{k1} + \sum_{n=2}^{\infty}\frac{1}{n}Q_{mn}(s)Q_{kn}(s) + s\sum_{n=1}^{\infty}\frac{1}{n}P_{mn}P_{kn}\right]. \tag{31}$$

The real part represents the effect of the fundamental mode at each side of the step, and the purely imaginary one, that of the higher order modes. Further dynamic corrections can be introduced as necessary.

VI. First Order Variational Solution

If we set $m = k = 0$ in (25), the latter becomes a scalar quantity and an analytical result can be recovered from (27), where we set

$$\eta_1 = \eta_2 = 1$$
$$G_1 = P_{00}$$
$$G_2 = Q_{00} = \sqrt{s}\,P_{00}. \tag{32}$$

Hence, we obtain from (27)

$$S_{11} = \frac{P_{00}^2}{Y_{00}} - 1 \tag{33a}$$

$$S_{22} = \frac{sP_{00}^2}{Y_{00}} - 1 \tag{33b}$$

$$S_{21} = S_{12} = \sqrt{s}\,\frac{P_{00}^2}{Y_{00}}. \tag{33c}$$

From (31) we have

$$\frac{Y_{00}}{P_{00}^2} = \frac{1+s}{2} + \frac{j\alpha us}{2} \tag{34}$$

where α is now a more accurate expansion for the capacitance of the step (see Fig. 2) than that of (2),

$$\alpha = k\left[\left(\frac{1}{3}+\frac{\frac{2}{3}}{1-\frac{3}{4}u^2}\right)\frac{J_{1/6}^2(\pi s)}{(\pi s)^{1/3}} + \sigma_2(s) + \sigma_1(1)\right] \tag{35}$$

which is a weak function of the step ratio s and frequency u and where

$$k = 2^{1/3}\Gamma^2\left(\frac{1}{6}\right)\Big/36 \approx 1.0849$$

$$\sigma_m(s) = \sum_{n=m}^{\infty}\frac{1}{n^2}\frac{J_{1/6}^2(n\pi s)}{(n\pi s)^{1/3}}, \qquad 0 < s \leqslant 1. \tag{36}$$

TABLE I
MODULES OF THE REFLECTION COEFFICIENT FOR TWO DIFFERENT HEIGHTS OF THE STEP ($s = 0.2, 0.8$) AND TWO VALUES OF FREQUENCY FOR A STANDARD X-BAND WAVEGUIDE

	$F = 8$ GHz			
S \ NY	1	2	3	4
0.2	0.6732	0.6731	0.6731	0.6731
0.8	0.1142	0.1126	0.1126	0.1126
	$F = 12$ GHz			
S \ NY	1	2	3	4
0.2	0.7091	0.7090	0.7090	0.7090
0.8	0.1283	0.1205	0.1204	0.1204

NY represents the numbers of basis functions used to approximate the field on the aperture.

VII. NUMERICAL RESULTS

An extensive numerical analysis has been carried out in order to ascertain some characteristics of the method presented in the previous sections. Salient features useful as guidelines and tests for numerical implementation are reported in this section. In particular, the cases of the single discontinuity, of two coupled discontinuities, and an example of a cascade of discontinuities are examined. The way in which the frequency dependence extraction and the quasi-static approximation affect the results has also been investigated.

The first case considered is that of the single discontinuity shown in Fig. 1. In this case, in order to investigate the convergence properties of the method, formula (27) has been used without extracting the frequency dependence. The error arising from this formula is due to the fact that a finite number of basis functions is selected (say N) and that infinite sums are truncated after M terms.

It should be noted that in the conventional modal-matching technique, the choice of N and M is critical and is related to the geometrical parameters of the structure, giving rise to the phenomenon of relative convergence, while in this case no such phenomenon occurs. In fact, once the value of M is high enough so that Green's function is well approximated and no ill conditioning is present, no relationship need be maintained between M and N and the geometrical parameter.

To investigate the number of terms necessary to obtain stable results, a high value of M has been selected, and the modulus of the reflection coefficient has been calculated considering $N = 1, 2, \cdots, 4$ terms. The corresponding results are given in Table I for two different values of the step ratio and the frequency. It is apparent that two terms are always sufficient to obtain very good results.

The convergence with respect to the number of terms retained when approximating the Green's function has been successively examined. In Table II, columns 1 and 2 are obtained by using only one basis function to represent the field ($N = 1$) and considering respectively only two and ten terms ($M = 2, 10$) of the sum (25). In the same table, columns 3 and 4 refer to the case of $N = 2$ when four and 80 terms are retained for the Green's function ($M = 4, 80$). The fast convergence of the sum and, consequently, the slight numerical effort required are evident. The last column of Table II reports the results obtained by using the expression given in [1, p. 307]. The agreement with the results of the fourth column ($N = 2$, $M = 80$) is almost perfect.

TABLE II
MODULUS OF THE REFLECTION COEFFICIENT, RELATIVE TO A WR90 WAVEGUIDE, FOR DIFFERENT VALUES OF s AND FREQUENCY

	$F = 8$ GHz				
S	$N=1$ $M=2$	$N=1$ $M=10$	$N=2$ $M=4$	$N=2$ $M=80$	[1]
0.2	0.6720	0.6730	0.6725	0.6731	0.6731
0.4	0.4364	0.4383	0.4377	0.4384	0.4384
0.6	0.2552	0.2565	0.2556	0.2561	0.2561
0.8	0.1124	0.1140	0.1123	0.1126	0.1126
	$F = 10$ GHz				
S	$N=1$ $M=2$	$N=1$ $M=10$	$N=2$ $M=4$	$N=2$ $M=80$	[1]
0.2	0.6838	0.6864	0.6851	0.6869	0.6869
0.4	0.4542	0.4596	0.4580	0.4600	0.4600
0.6	0.2666	0.2701	0.2678	0.2694	0.2694
0.8	0.1150	0.1196	0.1150	0.1157	0.1156
	$F = 12$ GHz				
S	$N=1$ $M=2$	$N=1$ $M=10$	$N=2$ $M=4$	$N=2$ $M=80$	[1]
0.2	0.7034	0.7080	0.7055	0.7090	0.7089
0.4	0.4852	0.4948	0.4921	0.4960	0.4959
0.6	0.2854	0.2917	0.2884	0.2915	0.2915
0.8	0.1188	0.1272	0.1191	0.1205	0.1203

N is the number of basis functions used, while M is the number of terms retained in the sum 25. The last column refers to the results from [1].

It is now possible to examine the effects of the frequency-dependence extraction described in Section V. Let us at same time consider the modification of the solution caused by the introduction of the quasi-static approximation. Fig. 5 shows the correct result obtained using two terms (dashed curve) together with the quasi-static approximation relative to one-term expansion ($N = 1$) and considering only one term dynamically (lower continuous curve). The upper continuous curve is relative to the simple circuit of Fig. 4(c). It should be noted that this comparison is done for the worst case, since a step ratio $s = 0.8$ is considered; for lower step ratios, the accuracy increases.

Two types of double interacting discontinuities frequently occur in practiced, namely the thick iris case and the stub case. From the point of view of numerical analysis, in addition to the previous parameters M and N, the number of accessible modes (P) should also be considered. Fig. 6 represents the modulus of the reflection coefficient relative to an iris of $s = 0.5$ and thickness

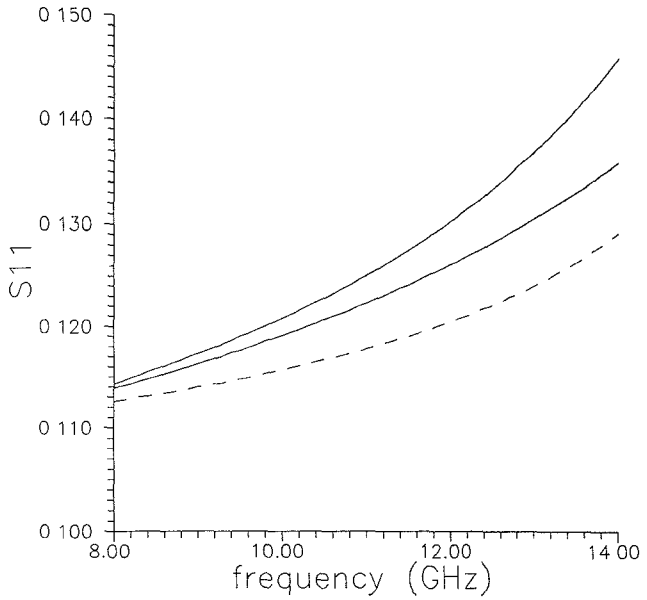

Fig. 5. Modulus of the reflection of a single step discontinuity (WR90, $s = 0.8$). Effects of quasi-static approximation and of the frequency dependence extraction. The dashed line is the solution obtained considering two basis functions; the other two curves refer to only one basis function. The upper one is obtained from the equivalent circuit of Fig. 4(c).

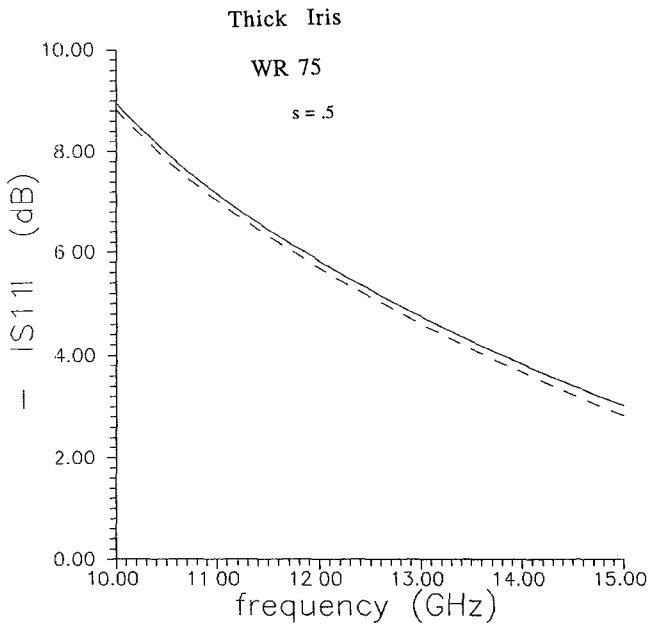

Fig. 6. Modulus of the reflection coefficient for a thick iris in a WR75 waveguide; $s = 0.5$ and the thickness of the iris is $d = 0.768$ mm. The continuous curve is obtained considering two basis functions and six "accessible" modes; the dashed one is obtained using the equivalent circuit.

$d = 0.768$ mm inside a WR75 waveguide. The curves reported in this figure are obtained by using $N = 2$ and 6 accessible modes ($P = 6$, continuous line). The very good approximation provided by the circuit of Fig. 4(c) is evident.

With regard to the stub case, the resonant nature of the two interacting discontinuities must be properly taken into account. To this end, it can be advantageous to consider the resonant cell from directions other than the propagating one. By doing so, excellent results can be obtained. Fig. 7 compares the computed (dashed line) and the measured (continuous line) modulus and phase of the scattering parameters for the structure in the inset. Only two basis functions have been used on the two apertures, and only three accessible modes have been considered. The excellent agreement between the computed results and the experimental data is evident.

As a last example, Fig. 8 compares experimental and calculated data for the three-stub structure shown in the inset. The latter further confirms how it is possible to obtain very accurate results with a modest numerical effort.

VIII. Conclusions

The problem of the *E*-plane step in rectangular waveguide has been reconsidered. The use of the appropriate edge condition, combined with a variational expression of the generalized scattering matrix, has led to a significant reduction of the numerical effort. In fact, as is evident also from a comparison with experimental data, inversion of a matrix of maximum size 2×2 is required to obtain the generalized scattering matrix.

Moreover, when the frequency extraction is used, new approximate circuits with frequency-independent elements are derived. The method outlined in the previous sections is therefore proposed as a valid improvement of the classical modal-matching routines, as well as of the equivalent circuits reported in [1].

Appendix I

The normalization of the Gegenbauer polynomials is given in [7, p. 827]:

$$\int_{-1}^{+1}(1-t^2)^{\upsilon-1/2}C_m^{\upsilon}(t)C_n^{\upsilon}(t)\,dt = \frac{\pi 2^{1-2\upsilon}\Gamma(2\upsilon+m)}{(m)!(m+\upsilon)\Gamma^2(\upsilon)}\delta_{mn} = 2N_m^2\delta_{mn}. \tag{A1}$$

With the choice $\upsilon = 1/6$, the normalization constant N_m appearing in (18) is then

$$N_m = \frac{2^{-1/6}}{\Gamma\left(\frac{1}{6}\right)}\left[\frac{\pi\Gamma\left(\frac{1}{3}+m\right)}{\left(m+\frac{1}{6}\right)(m)!}\right]^{1/2}. \tag{A2}$$

Coefficients of the expression (22) are as follows:

$$Q_{mn} = \int_0^d w\psi_n f_m\,dy = \frac{\sqrt{\epsilon_n}\sqrt{s}}{2N_m}\int_{-1}^{+1}\frac{\cos n\pi st}{(1-t^2)^{1/3}}C_{2m}^{1/6}(t)\,dt \tag{A3}$$

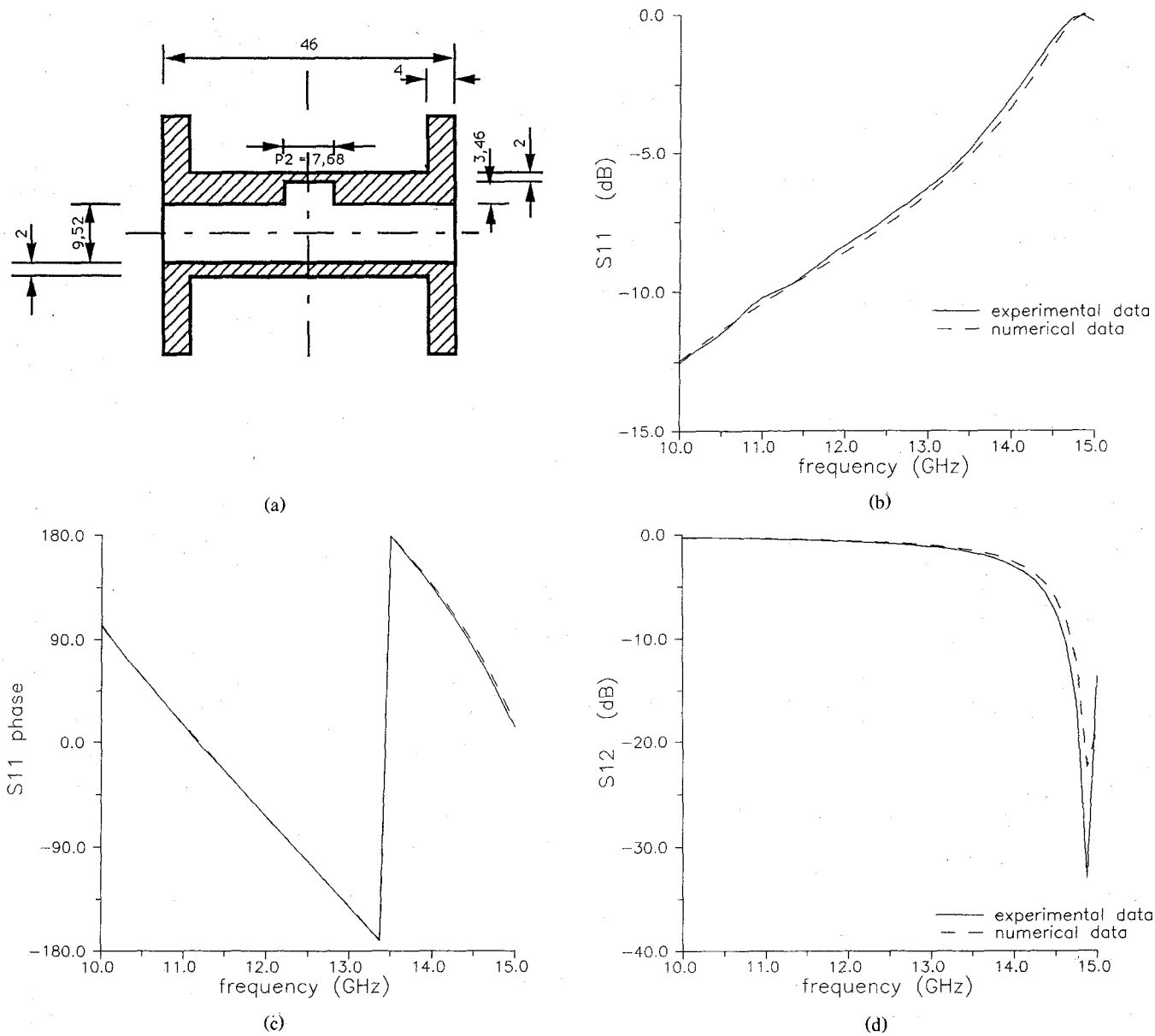

Fig. 7. Experimental and computed scattering parameters for the structure in Fig. 7(a), referring to a WR75 loaded with one E-plane stub. All dimensions are in mm.

where

$$\epsilon_n = 1, \qquad n = 0$$
$$= 2, \qquad n > 0$$

and s is the step ratio d/b. The above integral is recognized as the real part of the following standard integral [7, p. 830]:

$$\int_{-1}^{+1} (1-t^2)^{\upsilon-1/2} e^{j\alpha t} C_\mu^\upsilon(t)\, dt = \frac{\pi 2^{1-\upsilon}\Gamma(2\upsilon+\mu)}{\mu!\Gamma(\upsilon)} (j)^\mu \alpha^{-\upsilon} J_{\mu+\upsilon}(\alpha). \quad \text{(A4)}$$

Setting now $\alpha = n\pi s$ and $\mu = 2m$ in the above, we obtain

$$Q_{mn}(s) = \sqrt{2s}\, C_m \frac{J_{2m+1/6}(n\pi s)}{(n\pi s)^{1/6}}, \qquad n > 0 \quad \text{(A5)}$$

with

$$C_m = (-1)^m \left[\frac{\pi\Gamma\left(\frac{1}{3}+2m\right)}{(2m)!}\right]^{1/2} \left(2m+\frac{1}{6}\right)^{1/2}.$$

For $n = 0$, the limit of the Bessel function of small argument is

$$\lim_{z\to 0} \frac{J_\upsilon(z)}{z^\upsilon} = \frac{1}{2^\upsilon \Gamma(\upsilon)\upsilon}.$$

Hence for $\upsilon = 2m + 1/6$, we have

$$Q_{00} = \sqrt{s}\, \frac{2^{1/3}}{\Gamma\left(\frac{1}{6}\right)} \left[3\pi\Gamma\left(\frac{1}{3}\right)\right]^{1/2} = \sqrt{s}\, N_0$$
$$Q_{m0} = 0, \qquad m > 0 \quad \text{(A6)}$$

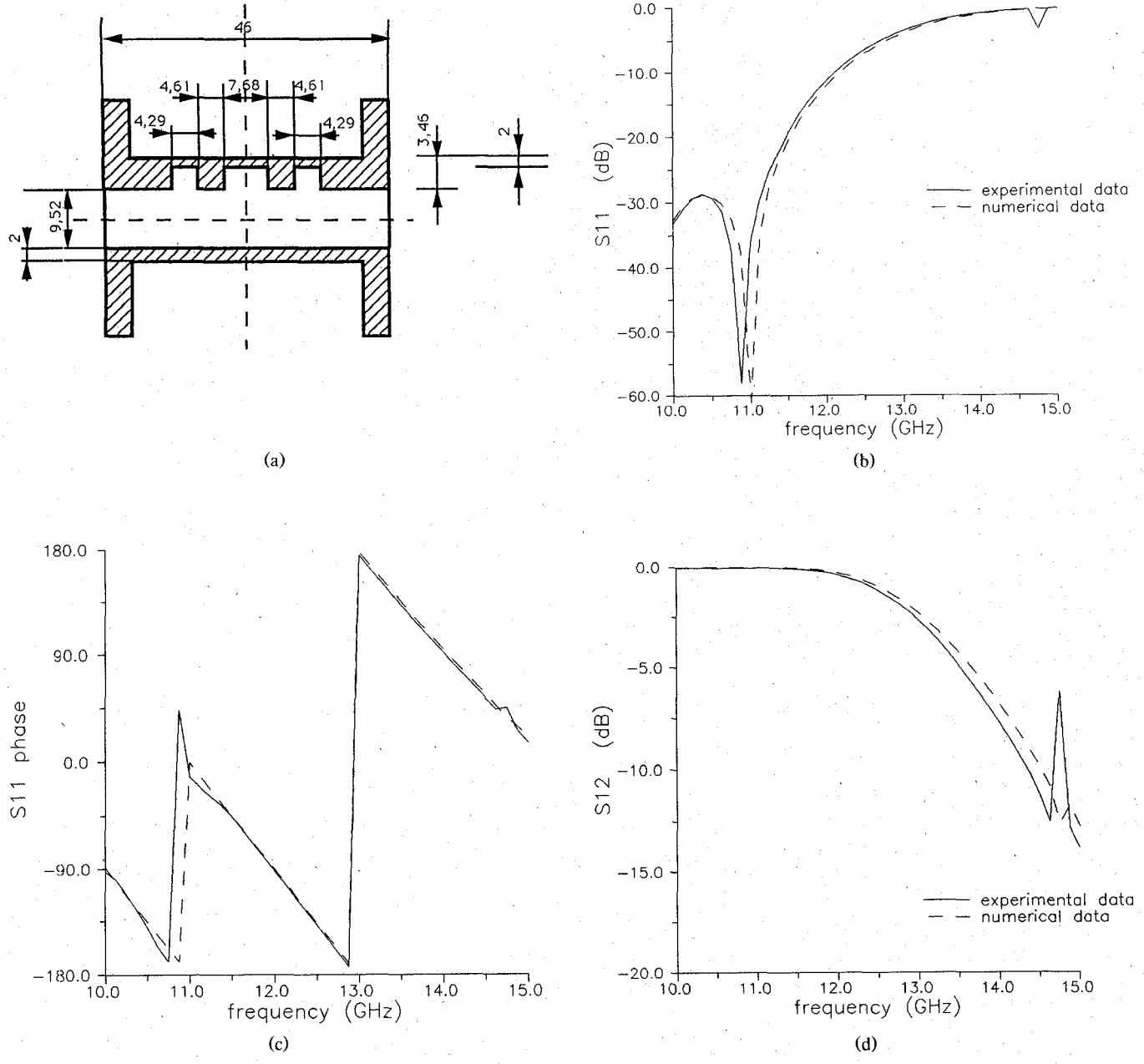

Fig. 8. Experimental and computed scattering parameters for the structure in Fig. 8(a) referring to a WR75 rectangular waveguide loaded with three *E*-plane stubs. All dimensions are in mm.

Returning now to the expression (20), its coefficients,

$$P_{mn} = \int_0^d W \varphi_n f_m \, dy$$

are obtained by setting $x = n\pi$ in A4; hence

$$P_{mn} = \sqrt{\epsilon_{nm}} \frac{J_{2m+1/6}(n\pi)}{(n\pi)^{1/6}} \tag{A7}$$

which are s-independent.

From the expansion of the Bessel function for large arguments,

$$J_v(z) \approx \sqrt{\frac{2}{\pi z}} \cos\left(z - \frac{\pi v}{2} - \frac{\pi}{4}\right)$$

it is noted that, for large n, we have

$$\frac{J_{2m+1/6}(n\pi s)}{(n\pi s)^{1/6}} \approx (-1)^m \sqrt{\frac{2}{\pi}} (n\pi s)^{-2/3} \cos \pi \left(ns - \frac{1}{3}\right). \tag{A8}$$

Hence series such as those appearing in (24) converge as $n^{-7/3}$.

Appendix II
Second-Order Variational Solution for Single Step

It is noted that the Gegenbauer polynomial C_0 represents exactly the field of the fundamental LSE_{10} mode. Consequently in Appendix I, $Q_{m0} = 0$ for $m > 0$. This fact allows the second-order variational solution for the single step also to be written down without matrix inversion. Let

$$Y = \begin{bmatrix} Y_{00} & Y_{01} \\ Y_{01} & Y_{11} \end{bmatrix}$$

be the resulting 2×2 matrix, and Z be its inverse. Then, we have

$$Z_{11} = \left[Y_{00} - Y_{01}^2 / Y_{11} \right]^{-1}$$

and, on account of (27),

$$S_{11} = \frac{P_{00}^2}{Y_{00} - Y_{01}^2 / Y_{11}} - 1$$

and similarly for the other elements of the two-port scattering matrix.

Acknowledgment

The authors, in particular the second author, would like to thank Prof. R. Sorrentino for providing the experimental data as well as for support and encouragement during this work.

References

[1] N. Marcuvitz, *Waveguide Handbook*. New York: McGraw-Hill, 1951, p. 308.
[2] T. Rozzi, "A new approach to the network modelling of capacitive irises and steps in waveguide," *Int. J. Circuit Theory and Appl.*, vol. 3, pp. 339–354, 1975.
[3] R. Mittra, T. Itoh, and T. S. Li, "Analytical and numerical studies of the relative convergence phenomenon arising in the solution of an integral equation by the moment method," *IEEE Trans. Microwave Theory Tech.*, vol. MTT-20, pp. 96–104, Feb. 1972.
[4] J. Schwinger and D. S. Saxon, *Discontinuities in Waveguides*. New York: Gordon and Breach, 1968.
[5] S. W. Lee, W. R. Jones, and J. J. Campbell, "Convergence of numerical solutions of iris-type discontinuity problems," *IEEE Trans. Microwave Theory Tech.*, vol. MTT-19, pp. 528–536, June 1971.
[6] R. E. Collin, *Field Theory of Guided Waves*. New York: McGraw-Hill, 1960, ch. 8, p. 335.
[7] I. S. Gradshteyn and I. M. Ryzhik, *Table of Integrals, Series and Products*. New York: Academic Press, 1980.

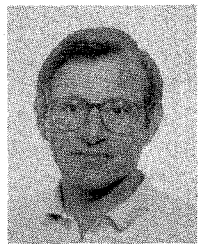

Tullio Rozzi (M'66–SM'74–F'90) received the degree of Dottore in physics from the University of Pisa, Italy, in 1965, the Ph.D. degree in electronic engineering from leeds University, U.K., in 1968, and the D.Sc. degree from the University of Bath, U.K., in 1987.

From 1968 to 1978 he was a Research Scientist at the Philips Research Laboratories, Eindhoven, The Netherlands, having spent one year, 1975, at the Antenna Laboratory, University of Illinois, Urbana. In 1978 he was appointed to the Chair of Electrical Engineering at the University of Liverpool, U.K., and subsequently was appointed to the Chair of Electronics and made Head of the Electronics Group at the University of Bath in 1981. From 1983 to 1986 he held the additional responsibility of being Head of the School of Electrical Engineering at Bath. Since 1986 he has held the Chair of Antennas in the Faculty of Engineering, University of Ancona, Italy.

In 1975 Dr. Rozzi was awarded the Microwave Prize by the IEEE Microwave Theory and Technique Society. He is a fellow of the IEE (U.K.).

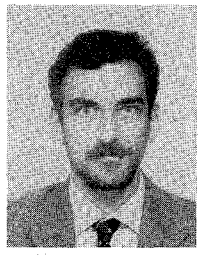

Mauro Mongiardo received the degree of Dottore in electronics engineering in 1983 in Rome.

Since then he has been involved in research on biological microwave radiometry and antenna inverse problems. He spent the year 1988 at the University of Bath, U.K., and since 1989 he has been a researcher at the University of Rome "Tor Vergata." His current research interests include the analysis and synthesis of passive microwave and millimeter-wave structures.